AFFDL-TDR-65-35

PRESSURE PROBE AND SYSTEM FOR MEASURING LARGE BLAST WAVES

J. RAY RUETENIK and S. DEAN LEWIS

MASSACHUSETTS INSTITUTE OF TECHNOLOGY

TECHNICAL REPORT AFFDL-TDR-65-35

JUNE 1965

AIR FORCE FLIGHT DYNAMICS LABORATORY
RESEARCH AND TECHNOLOGY DIVISION
AIR FORCE SYSTEMS COMMAND
WRIGHT-PATTERSON AIR FORCE BASE, OHIO

This Document Contains
Missing Page/s That Are
Unavailable In The
Original Document

OR are
Blank pgs.
that have
Been Removed

NOTICES

When Government drawings, specifications, or other data are used for any purpose other than in connection with a definitely related Government procurement operation, the United States Government thereby incurs no responsibility nor any obligation whatsoever; and the fact that the Government may have formulated, furnished, or in any way supplied the said drawings, specifications, or other data, is not to be regarded by implication or otherwise as in any manner licensing the holder or any other person or corporation, or conveying any rights or permission to manufacture, use, or sell any patented invention that may in any way be related thereto.

Copies of this report should not be returned to the Research and Technology Division unless return is required by security considerations, contractual obligations, or notice on a specific document.

300 - July 1965 - 448-51-1120

PRESSURE PROBE AND SYSTEM FOR MEASURING LARGE BLAST WAVES

J. RAY RUETENIK and S. DEAN LEWIS

MASSACHUSETTS INSTITUTE OF TECHNOLOGY

FOREWORD

This report was prepared by the Aeroelastic and Structures Research Laboratory of the Massachusetts Institute of Technology, Cambridge, Massachusetts, under Air Force Contract No. AF 33(616)-8499, Project No. 5710, "Nuclear Weapon Effects Research and Testing." Dr. Ruetenik served as project leader and Professor Emmett A. Witmer as supervisor of the work covered under this contract. The work was administered under the direction of the Air Force Flight Dynamics Laboratory, Research and Technology Division, with Mr. Edward Pugh the project engineer.

The contractor's report number is 105-2.

The cooperation of Mr. Pugh and his group toward the success of this investigation is gratefully acknowledged. The program of measurements in the field was carried out at Edwards Air Force Base by Aircraft Armaments, Inc., Cockeysville, Maryland under the supervision of Mr. William Schuette, and the support of EAFB personnel, with Mr. John Rievley, the AFFDL engineer, in charge.

Manuscript released by authors January 29, 1965 for publication as an RTD Technical Report.

ABSTRACT

A new pancake-type pressure probe was developed for the measurement of blast pressure waves during the BIG SEA sled tests. This probe employs transducers of the type selected for wing pressure measurements in that program. It was evaluated in the shock tube under a range of flow Mach numbers encountered during the test. From these shock tube tests, a probe form calibration was determined.

Application of this type of probe to the BIG SEA tests is also described, including the mounting system, transducer and electronic calibration, and one blast wave record derived from this type of probe is presented. The results of the shock-overpressure measurements are compared with other test data.

The pancake probe has a diameter of 4 inches and a thickness of 0.5 inch. The accuracy of measurement has been determined to be 3-5% of the shock overpressure for blast waves where the positive duration is 10 milliseconds or greater. The response time has been found to be less than 0.7 milliseconds.

PUBLICATION REVIEW

This report has been reviewed and is approved.

RICHARD F. HOENER
Acting Chief, Structures Division
Flight Dynamics Laboratory

TABLE OF CONTENTS

LIST OF ILLUSTRATIONS

LIST OF SYMBOLS

a	Local sonic velocity
C	Coefficient in Eq. (3)
d	Probe or cylinder diameter
f_R	Reflection factor based on Goodman[1] empirical curve for free-air pentolite
M	Particle Mach number
p	Pressure
$\tilde{p}$	Pressure as measured by probe
p_w	Pressure as measured at shock-tube wall
Δp	Blast overpressure
Δp_s	Shock overpressure
$\bar{P}$	Ratio of ambient pressure to 14.7 psi.
P_{21}	Shock pressure ratio, p_2/p_1
q	Dynamic pressure, $1/2\ \rho u^2$
R	Distance from charge center to probe transducer, ft.
R_e	Probe Reynolds number, ud/ν
R_0	Distance from charge center to track centerline at 9000 ft. station, ft.
S,d	Coordinates of vertical pipe support relative to 9000 ft. station, ft. (see Fig. 8)
t	Time
t''	Time referred to sled arrival at 20-millisecond trip

$\Delta t_{+\Delta p}$	Positive-overpressure duration of blast wave
u	Particle velocity
W	Charge weight, lb. of explosive
$\overline{W}$	Effective charge weight, lb. of pentolite
β	$\sqrt{1-M_2^2}$
ρ	Density
γ	Kinematic viscosity

Subscripts

0	Ambient conditions
1	Conditions ahead of shock in shock tube
2	Conditions behind shock in shock tube

SECTION I

INTRODUCTION

During the first portion of the BIG SEA program[1] of blast experiments conducted at Edwards Air Force Base, it was found that the calibrations of the piezo-electric pressure probes which were in use for measuring the blast overpressure were not repeatable. This problem was also evident in the scatter of the blast data that were obtained. Therefore, the pressure probe, described in Section II, was developed for these blast measurements.

A pancake configuration was selected for the probe, similar to the configuration employed by the Army Ballistic Research Laboratory, except that the thickness was increased from 0.25 to 0.5 inches in order to accommodate the pressure transducer that was available. The diameter of the probe was increased from 3 to 4 inches to keep the thickness ratio down to 12.5 percent, but this thickness ratio is still relatively large, so the probe was calibrated in the shock tube where an accurate calibration could be obtained. The aerodynamic response time for a probe of this size was expected to be a point of concern, so the response time was also measured in these shock-tube tests. These tests are described in Section III, and the results are discussed with reference to the accuracy that was achieved in the blast measurements carried out in the BIG SEA program.

The technique that was devised for measuring the blast overpressure in the field is presented in Section IV, and the results from shock-overpressure measurements in the BIG SEA tests using this equipment are presented and discussed with reference to previous measurements that were collected by Goodman[2].

Recommendations for modification of this probe for future tests are discussed.

SECTION II

GENERAL

2.1 Description of Pressure Probe

A sketch of the probe is shown in Fig. 1. It has a pancake configuration with a four-inch diameter and 0.5-inch thickness. Two Bytrex semiconductor strain-gage-type pressure transducers Model No. HF-100 are mounted on the opposite faces. These particular transducers were selected because they had been used successfully in the BIG SEA program for measuring the pre-blast and blast-induced pressures on wings, and they had exhibited a high degree of accuracy, stability, and repeatability.

In blast experiments, the plane of the probe is oriented in a vertical plane with the axis through the stem of the probe being directed toward the center of the explosive as shown in Fig. 2. The transducers are displaced laterally from this axis in order that the probe be as thin as possible. The leads from the transducers are fed out through a passage in the sting of the probe.

2.2 List of Calibrations

Three types of calibrations were made of the probe system:

1. Probe Form Calibration. A probe acts as a disturbance to the blast-induced flow, so it is necessary to determine a relationship between the probe-measured pressure and the undisturbed blast (free-stream) pressure. This calibration was made in the MIT 8 x 24-inch shock tube, and is described in Section III.
2. Pressure Transducer Calibration. Each pressure transducer is in a bridge circuit to its amplifier. The

pressure transducers were calibrated in the probe while in position by applying pressure to each transducer and comparing the amplifier output against the output obtained when precision resistors were inserted in the bridge. Thus the transducers were calibrated against the resistors. This calibration was made before and after every run in the laboratory and the field.

3. Amplifier and Recorder Calibration. A few seconds prior to each test in the field, the precision resistors were switched into the bridge circuits to calibrate the electronic system. These signals were placed at the beginning of the recorder tapes, thereby providing an in-run calibration in the field.

All three calibrations must be made to assure successful measurement of the pressure. Further details of the calibrations are given in Sections III and IV.

SECTION III

LABORATORY TESTS

3.1 Test Setup

In a steady-state flow, the pressure probe would be calibrated as a function of Mach number, and perhaps, Reynolds number. For measurements in a blast wave, the effect of the diffracting shock wave and time-dependent flow field must be determined. Accordingly, the probe was calibrated in the MIT 8 x 24-inch shock tube where both the "steady-state" and transient calibrations could be determined in the same set of tests.

A photograph of the probe, in the shock tube, is shown in Fig. 3. The probe was oriented with the pancake horizontal to minimize the wall interference. A special sting was built to position the probe well ahead of the cross-support in order to delay the arrival at the sensor of the shock reflected from the downstream cross-support; the calibration period was terminated when this reflected shock reached the probe.

A sketch of the test setup in the shock tube is shown in Fig. 4. The objective of the tests was to compare the pressure measured by the probe against the well-defined pressure behind the shock wave. The shock overpressure was measured by a Bytrex pressure transducer located in the wall of the shock tube 12.2 inches ahead of the center of the sensing area of the probe, well upstream of the probe disturbances. The shock velocity and strength were determined by measuring the difference in the shock arrival time at two Schlieren light screens on a 3-ft. spacing ahead of the probe, and were checked against measurement of the shock overpressure.

The pressure signals were recorded on a Tektronix 551 dual-beam oscilloscope. Typical oscilloscope traces are shown in Fig. 5. The wall pressure, p_w, was recorded on the upper beam, and the difference between the probe-measured pressure, $\tilde{p}$, and wall pressure was recorded on the lower beam; the latter is the calibration quantity, so the sensitivity was made 5 times greater than for the upper beam in order to increase the accuracy. On the oscillograph records, it is evident that the lower beam is driven off-scale when the shock reaches the wall transducer, and returns on-scale when the shock reaches the probe transducer.

The initial pressure, p_1, in the shock tube was 31 inches Hg., approximately one atmosphere, in most of the tests. A few runs were made with an initial pressure of 5 in. Hg., with the hope of being able to extend the tests to higher Mach numbers within the shock-tube pressure capability; it turned out that the latter data departed from the one-atmosphere data at transonic speeds, so the sub-atmospheric tests were abandoned. The Mach number of the shock-induced flow, M_2, varied from 0.15 to 0.76.

3.2 Probe Form Calibration

It turns out that the probe has a response time (until signal remains within $\pm$ 0.05 Δp_s of steady state) of 0-0.7 milliseconds. Therefore, the first millisecond of the probe traces $\tilde{p}-p_w$ was ignored, and the probe calibration was obtained from a faired curve of the trace for the next 2 milliseconds. The traces had a peak-to-peak oscillation of about 10 percent of the shock overpressure, Δp_s, and it is estimated that the trace could be faired to about 0.03 Δp_s. For all of the test data, the ratio $(\tilde{p}-p_w)/(p_2-p_1)$ is plotted in Fig. 6a as a function of M_2.

A calibration curve was obtained as a function of the flow Mach number M by using the Prandtl-Glauert relation for subsonic flow giving

$$\frac{\tilde{p}-p}{q} = \frac{C}{\beta} \qquad (1)$$

where q is dynamic pressure, C is a constant to be determined, and $\beta = \sqrt{1-M^2}$. Equation (1) would be expected to apply under conditions of steady-state flow provided the speed is below the critical Mach number and Reynolds number effects are not significant. The data in Fig. 6a are presented in terms of the pressure jump across the shock, p_2-p_1, and the properties behind the shock front, for which Eq. (1) becomes

$$\frac{\tilde{p}-p_w}{p_2-p_1} = \frac{C}{\beta_2} \quad \frac{q_2}{p_2-p_1} \qquad (2)$$

In Fig. 6b, the calibration lines identified in Fig. 6a appear as straight lines, based on changing Eq. (2) as follows:

$$\frac{(\tilde{p}-p_w)\beta_2}{q_2} = C \qquad (3)$$

At subsonic speeds below the critical Mach number, the best fit to the data was obtained with C = -0.22. The critical Mach number for $p_1 \approx 1$ atmosphere appears to be M = 0.55. Above the critical Mach number, the data were fitted by taking C as a linear polynomial in M_2, giving

$$C = -0.22 \qquad M_2 \leq 0.55$$
$$= -0.44 + 0.4\, M_2 \qquad 0.55 \leq M_2 \leq 0.75 \tag{4}$$

The standard deviation of the data in Fig. 6a from this curve is 0.02, which indicates that the previous estimates of $\pm$ 0.03 Δp_s for the accuracy of fairing the traces is about right.

To apply the probe form calibration obtained in the shock tube to measuring the pressure in a blast wave, the instantaneous quantities M, β, and q would be used in place of the properties M_2, β_2, and q_2 for the shock tube. Specifically, Eq. (1) would be employed where C is obtained from Eq. (4) with the subscript 2 suppressed. In this regard, it should be pointed out that the probe does not have an instantaneous response, so the instantaneous quantities must be employed with regard to the finite response time, which will be discussed below.

It should be noted that the effect of Reynolds number is not specifically included in this calibration. The Reynolds number is expected to have a negligible effect for subsonic flow. But, for a given initial pressure, the Reynolds number is a function of Δp_s, and approximately decays as a function of Δp until the arrival of the contact surface. Therefore, the Reynolds number is implicit in the Mach number (or overpressure) dependence of the probe form calibration. At transonic speeds ($M > 0.55$) there was an effect of the initial pressure on the probe form calibration and this is interpreted as a Reynolds number effect. Therefore, at transonic speeds, the calibration given by Eq. (3) has an implicit Reynolds number effect which is approximately prescribed by the initial pressure.

3.3 Probe Response Time

The pressure transducer has a response time of 50 microseconds[3], but the time required for the flow surrounding the probe to come to equilibrium is considerably longer. The latter response time, which could be called the aerodynamic response time, has been determined and will now be discussed.

The 5 traces of $p-p_w$ in Fig. 5 are typical of the results of the shock-tube tests. A curve was faired through the traces, and it was found that the faired curve would attain to within 5 percent of the steady-state value within 0.7 milliseconds. There was no particular trend in the response time with Mach number; in fact, it was difficult to determine the response time with much accuracy because of the oscillation in pressure due to the diffraction of the shock wave and succeeding rarefaction and shock waves -- particularly at the higher shock strengths. In view of this uncertainty, the aerodynamic response time was given the nominal value of one millisecond; accordingly, the first millisecond of each trace was ignored in both the calibration and blast records.

The aerodynamic response time can also be estimated by using indicial-sinking theory. If a circular cylinder is suddenly set in motion normal to its axis at a constant speed, the indicial-sinking theory of Miles[4] indicates that the loading on the cylinder would reach essentially steady state in the time $\Delta t'_R$ where

$$\frac{a\Delta t'_R}{d} = 3 \qquad (5)$$

a is the speed of sound, and d is the cylinder diameter. If, to estimate the response time of the probe, d is taken as the probe diameter and a = 1100 to 1300 fps, then $\Delta t_R' \approx$ 1 msec., which agrees with the measured response time for the shock diffraction.

The response time is a principal factor affecting the accuracy in determining the shock overpressure from the pressure records. This is shown in the figure below where the response time is indicated as Δt_R.

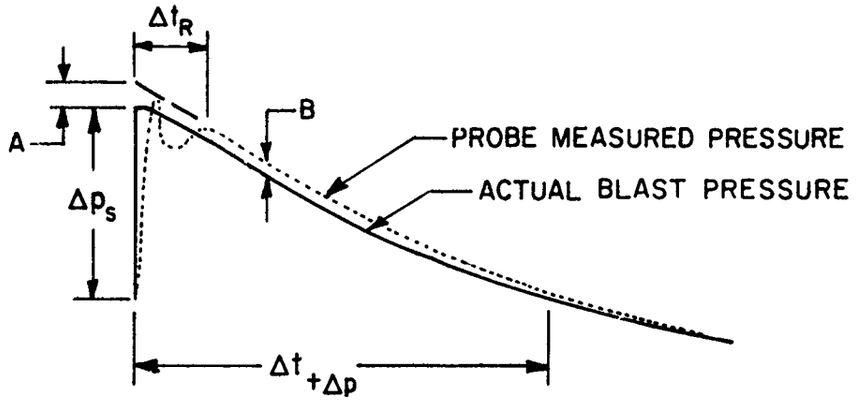

The shock overpressure is determined by extrapolating the recorded overpressure data in the period immediately following Δt_R to the shock arrival time. The error in this extrapolation, indicated as A in the sketch, is due to the combined effects of two factors: (1) the uncertainty associated with extrapolating the data over the time interval Δt_R (even if B is zero), and (2) the offset in the extrapolation due to B, which arises from the pressure lag during the decay period.

The error B, during the decay period, can be estimated by assuming that the probe responds as a first-order system for which the time constant would be equal to one-third of the response time, i.e., $\Delta t_R/3$. By approximating the decay as a straight line, the error is

$$\frac{B}{\Delta p_s} = \frac{\Delta t_R}{3\Delta t_{+\Delta p}} \qquad (6)$$

To keep this error B within 0.03 Δp_s, it is necessary that $\Delta t_{+\Delta p} > 10$ msec. for $\Delta t_R = 1$ msec. This is the error estimate for the decay period of the blast wave, after the probe has responded to the shock and before the contact surface arrives.

The error A in the extrapolation of the overpressure for short duration blasts can now be estimated. For $\Delta t_{+\Delta p} = 10$ msec., A is 5 percent of Δp_s; 3 percent due to B, and 2 percent due to the extrapolation.

The result is that the probe can be expected to have a 5 percent accuracy in blast measurements, so long as $\Delta t_{+\Delta p} > 10$ msec. For shorter blast durations, it would be advisable, (a) to reduce the probe diameter in order to reduce the aerodynamic response time, and (b) to reduce the thickness ratio in order to reduce the magnitude of the probe error $\tilde{p}$-p.

SECTION IV

FIELD TESTS

4.1 Blast-Line Setup

The probe was employed in the BIG SEA program to measure the HE-produced blast wave in aircraft/nuclear-blast simulation experiments. The technique that was developed to use the probe in the blast tests in the field and the results of these tests are described in the following.

Each probe was attached to a horizontal sting, which extended the probe about 2 feet ahead of a vertical support pipe installed in a concrete base, Fig. 7. The probe sting was attached to the support pipe by a clamp which was streamlined to minimize shock reflections upstream to the probe. The probe was aligned to the HE charge as shown in Fig. 7.

A photograph of one blast-line pressure probe used in a typical test is shown in Fig. 2. Ten probes were employed per run. The probe array for each of the 9 runs of the BIG SEA program in which these probes were used is given in Table 1 for the ground plan shown in Fig. 8.

The accompanying electronic equipment was housed in a steel box, fabricated of 1/4-inch steel plate, partially buried in the site area. The top of the box was nearly flush with the surface of the ground. The box contained the amplifiers, tape recorder, power supplies, automatic calibration unit, timing receiver, and control unit. A photograph of this box is shown in Fig. 9. In most cases the wires from the probe to the box were buried for blast isolation. The tape recorder and timing receiver were shock-mounted in the box.

The electronic system for each probe is shown schematically in Fig. 10. For nine probes in each run the circuit shown in Fig. 10a was used, where the two signals from each probe were amplified and summed; the reason for summing the signals was to minimize the effect of flow direction, or probe alignment, on the overpressure measurement. For one probe in each run, the circuit shown in Fig. 10b was used, where the signals from each transducer were amplified and recorded separately; in this way the overpressure could be determined from the sum of the two signals and the flow direction could be determined from the difference.

The signals were saturation recorded on a 14-track Leach MTR-1200 magnetic tape recorder using a 54-kc. center frequency with 40% deviation. The tape speed was 60 ips. in record mode, and 30 ips. in playback mode. A 100-kc compensation signal was recorded on one track of each head, which reduced the wow-and-flutter signal to about 1 percent of the full band deviation.

4.2 Pressure-Transducer Calibration

For the transducer pair of each probe when used in combined fashion, the amplifiers were equalized and the output was balanced. The pressure transducers were calibrated against the precision resistors having nominal values of 25, 50, 75, and 100 percent of full-scale pressure. The calibrations were made before and after each run.

A typical calibration is shown in Fig. 11. The pressure was applied to each transducer, and the calibration data were least-square fitted with a straight line. The precision resistors of the in-run calibration system were then individually switched into the transducer bridges to obtain the equivalent

pressure for each resistor, including the value with no resistor. The pre-run and post-run calibrations were averaged to provide a calibration. This comprised the pressure transducer calibration (which is independent of the amplifiers and recorders).

4.3 In-Run Calibration and Event Sequence

The event sequence during a typical field test is discussed with reference to Fig. 12, which is a sketch of the tape-recorder signals for a pressure-transducer track and a timing track. The tape recorder has a two-minute record duration at a tape speed of 60 in. per second. Shortly after the recorder was started, the in-run calibration system was sequenced through the calibrate cycle, switching in the precision resistors for the 5-step (nominal 100, 75, 50, 25, and 0 percent of full-scale pressure) in-run calibration of the recorder tape.

After the calibrate sequence was completed for all of the recorders located on both the sled and the blast line, the sled-start was initiated. When the sled reached a pre-selected pair of screen boxes along the track, the blast was initiated. The time base, which is shown as the lower track in Fig. 12, was recorded on a separate track of each recorder. The signal was initially at the "off" level on this track. When the sled reached a second pair of screen boxes, called the 20-millisecond trip, the signal level on the time track was switched to the "on" level simultaneously on all recorders to provide a common time origin. The time code rode on the "on" level. Time after the 20-millisecond trip has been given the symbol t".

4.4 Data Reduction

The tapes were processed in the A/D conversion at a 50-microsecond sampling rate and the three calibrations (probe, pressure transducer, and in-run calibrations) were introduced to give a digitalized tape output in terms of blast overpressure. The pressure history was then machine plotted for each probe as shown in Fig. 13.

The pressure history in Fig. 13 is typical of the blast-line results. The shock front arrived at t" = 17.05 msec., and decayed fairly smoothly until unidentified waves arrived at t" = 25 msec. The second shock from the HE detonation arrived at t" = 37 msec. The arrival of the bow wave from the sled was predicted to be at t" = 44.6 milliseconds, and is identified in the figure.

4.5 Field-Test Results

The whole period of positive overpressure of a blast wave is generally important in blast-loading experiments. But Goodman[2] has collected data of the shock overpressure for free-air blasts using Pentolite in a large number of tests. Therefore, it was desired to compare the measurements of the shock over-pressure in the present tests with the data of reference 2, recognizing that this is only a comparison of data at the shock front, but that it was the only large collection of experimental data available for this comparison. The errors in the pressure measurement are expected to be greatest in determining the shock overpressure, for the reasons mentioned above, so that the evaluation of the probe errors at the shock front should provide a conservative indication of the probe accuracy.

Before proceeding with the comparison, it should be noted that there is a large scatter in the shock overpressure ratio data presented by Goodman; this amounts to as much as $\pm$ 25% at the shock strengths of interest, so that these data should be used primarily to indicate the trend of the overpressure variation with blast radius. In fact, Goodman empirically fitted an equation to these data which will be useful for this comparison.

The shock overpressure, Δp_s, was obtained for each probe, as described above, by extrapolating the data after the first millisecond from shock arrival back to the shock arrival time. The shock overpressure ratio, $\Delta p_s/p_1$, is plotted in Fig. 14 as a function of the reduced charge radius, $R(\overline{P}/W)^{1/3}$, for all of the probes used in Runs 5-8 of the BIG SEA tests, where W is the weight of the charge. No adjustment has been made to these data as presented in Fig. 14 for a slightly greater yield of Pentolite than TNT, which is given as 10 percent by Baker and Schuman[5], a 3 percent effect on the reduced charge radius.

The empirical curve obtained by Goodman[2] for free-air Pentolite blasts is plotted in Fig. 14, and also a curve representing perfect reflection of a "Goodman" Pentolite charge, which corresponds to a reflection factor, f_R, of 2. The data of the BIG SEA tests lie relatively close to the $f_R = 2$ curve, and the spread of the data in the region of high data density is noticeably less than for the data presented in Reference 2.

The above comparison is encouraging, but it is possible that the scatter between measurements in any one run might be even less, due to a difference in the yield/weight ratio between runs. To determine the radial and spherical consistency of the shock overpressure data on a run-by-run basis, the effective (Goodman) yield was computed in each run by computing

the yield that Goodman's empirical curve would give for the shock overpressure measured by each probe and averaging the values for a run to give an effective yield, $\overline{W}$, for each run; this value is tabulated in Table 2 in terms of a reflection factor, which is the ratio

$$f_R = \frac{\overline{W}}{W} \quad \text{for Pentolite}$$

$$= \frac{1.1\,\overline{W}}{W} \quad \text{for TNT} \qquad (6)$$

The 1.1 factor between the yield of Pentolite and TNT was taken from Reference 5. With this yield $\overline{W}$, Goodman's empirical equation was then used to compute a shock overpressure for each probe, called Δp_s (Goodman). The standard deviation of Δp_s as measured, to Δp_s (Goodman) was computed and tabulated in Table 2. It ranged from 3.7 to 6.6 percent in these runs.

This spread of the data in the field tests is about what would be expected with the 3-5 percent accuracy that was determined from the laboratory tests described above, and indicated that no important additional errors have entered in the field tests. Actually, the error in the shock-overpressure measurements may be even less, because any variation of the blasts in spherical symmetry or radial decay rate from Goodman's empirical equation would increase this number; however, it should be noted that there was no detectable trend of departure noted in these runs, except for a test (run F2) where the charge consisted of 8-lb. blocks of TNT in a 216-lb. stack and the blast was definitely nonspherical.

SECTION V

DISCUSSION

The probe that was developed should be useful for a wide range of blasts. It has an accuracy of 3-5 percent, referred to shock overpressure, for blasts where the positive-overpressure duration is at least 10 milliseconds, which is satisfactory for many tests. It has been calibrated up to shock strengths of $P_{21} = 3$.

However, the probe was developed in a relatively short time, and there are some improvements that could be made in the probe for future tests. This will be discussed with reference to the traces in Fig. 5.

There are large oscillations in the probe pressure immediately after shock arrival, particularly at the higher Mach numbers. The period of the oscillations is about 0.6 milliseconds. These oscillations are attributed to the diffraction of the initial shock and succeeding shocks and rarefaction waves over the probe. The magnitude of the oscillations is expected to be proportional to thickness ratio of the probe, so it would be useful to reduce the thickness of the probe in order to reduce the oscillations in the pressure signal.

The aerodynamic response time of the probe is expected to scale with the probe size; therefore, it would be worthwhile to reduce the probe diameter. Of course, reducing the probe diameter would increase the thickness ratio, which would increase the error in the pressure signal. So, it would be useful to test several probes with different diameters, all having a minimum thickness, to determine which gives the best overall performance.

Above 4 milliseconds after the shock reaches the probe, there is a large fluctuation in the signal that is attributed

to the reflection of the shock from the probe support. This interference signal increases markedly with shock strength; at $P_{21} = 3.05$ it is about 20 percent of Δp_s. Therefore, attention should be given to the support pipe that supports the probe sting in the field. The cross piece that supports the sting in the shock tube is about the same diameter as the support pipe used in the field. The coupling between the sting and the cross piece in the shock tube is more streamlined than the clamp used in the field, but the interference in the shock tube is increased somewhat by the confinement of the walls.

All of these problems increase as the shock strength is increased. It would be worthwhile, therefore, in future test programs to consider modifying the probe and support system to achieve greater accuracy with the probe in shock overpressure measurements, particularly for shock strengths greater than 2 and positive overpressure durations less than 10 milliseconds.

SECTION VI

CONCLUSIONS

Based on the tests of the probe in the shock tube and use of the probe in the BIG SEA tests, the following conclusions are made for shock overpressure measurements in the region of the blast between the shock front and the contact surface up to a flow Mach number of 0.75.

1. The accuracy for overpressure measurements is about 3 percent, except at the shock front, for blasts with positive overpressure durations of more than 10 msec.
2. The accuracy for shock overpressure measurements is about 5 percent for positive overpressure durations of more than 10 msec.
3. The aerodynamic response time of the present probe ($\pm$ 5 percent of step pressure) is about one millisecond.
4. The accuracy of the probe could be improved by reducing, (a) the probe thickness ratio, which would reduce proportionately the magnitude of the calibration, and, perhaps, (b) the probe diameter, which would reduce proportionately the response time.

REFERENCES

1. Wolf, I.O., et.al., An Experimental Investigation of Blast-Induced Airloads and Response of Lifting Surfaces. AFFDL-TR-64-176, August 1964.

2. Goodman, H.J., Compiled Free-Air Blast Data on Bare Spherical Pentolite. BRL Report No. 1092, February 1960.

3. Ruetenik, J.R., Laboratory Tests of Three Pressure Transducer Systems for BIG SEA Sled Test Program. MIT, Aeroelastic and Structures Research Laboratory, November 1961.

4. Miles, J.W., Transient Loading of Slender Bodies of Revolution. U.S. Naval Ordnance Report 2052, Inyokern, California, 1953.

5. Baker, W.E. and Schuman, W.J. Jr., Air Blast Data for Correlation with Moving Airfoil Tests. BRL TN 1421, August 1961.

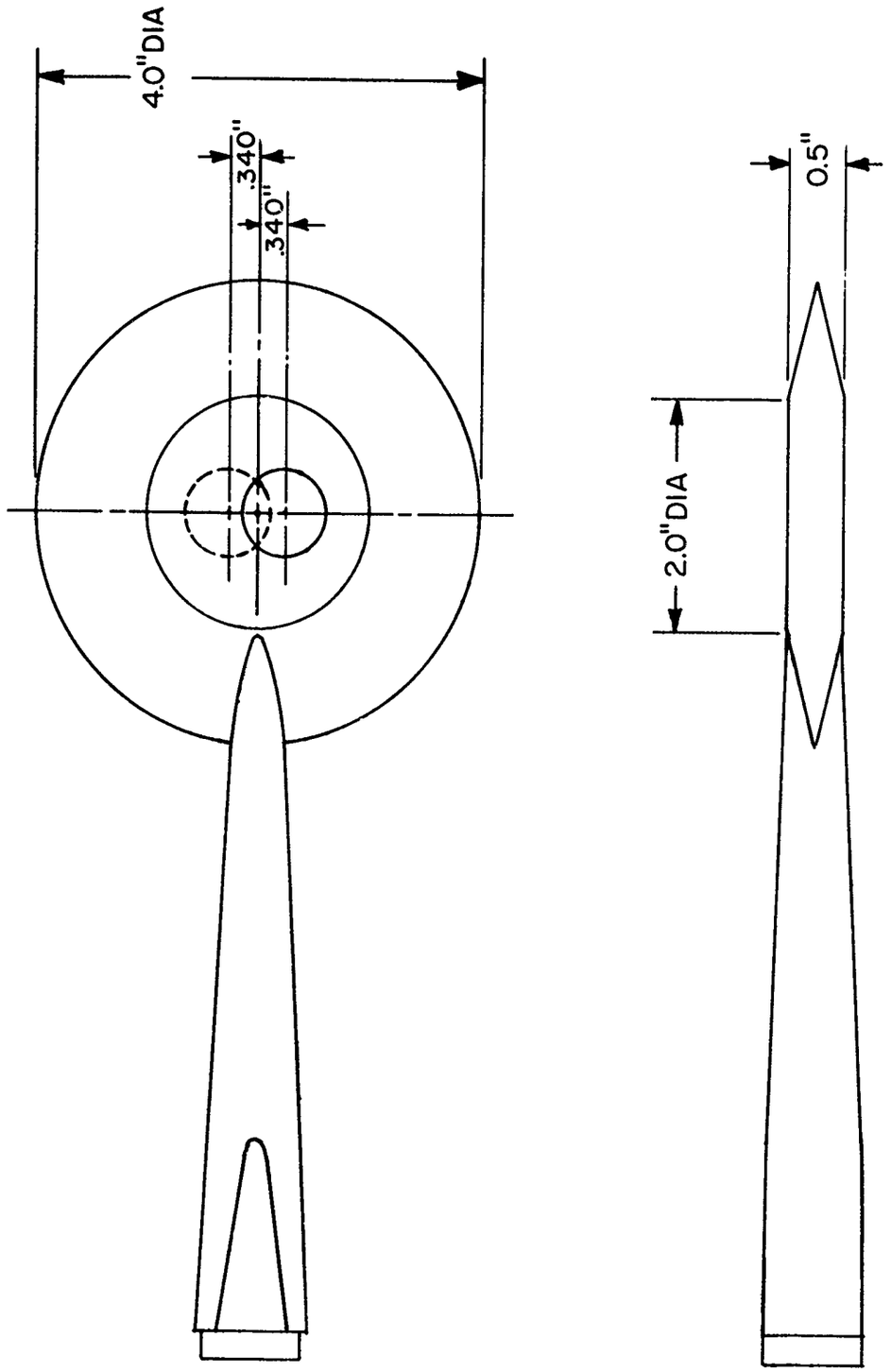

Figure 1 Sketch of Blast-Line Pressure Probe

Figure 2 Photograph of Blast-Line Pressure Probe Mounted Facing 12,000 Pound TNT Charge

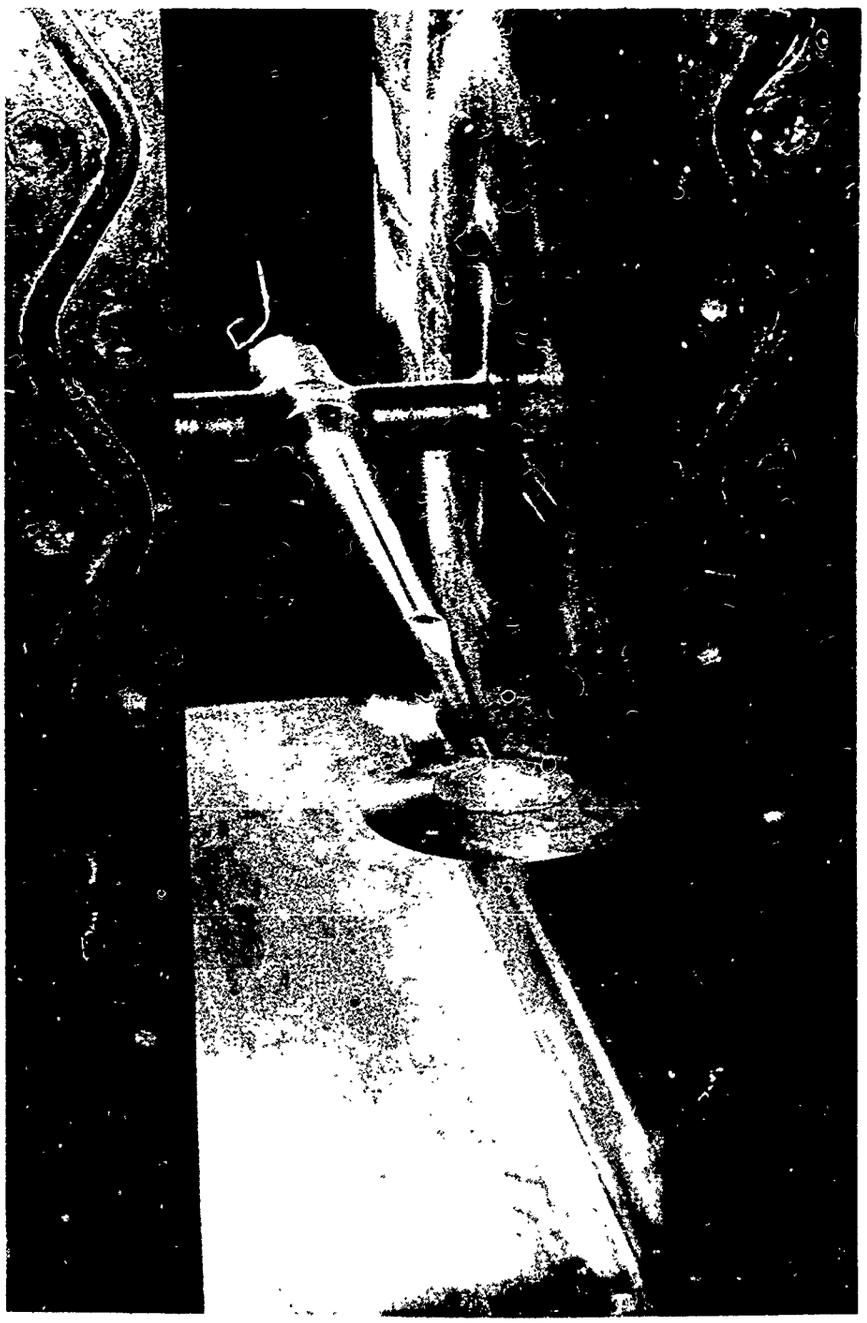

Figure 3 Blast-Line Probe Mounted in Shock Tube for Calibration

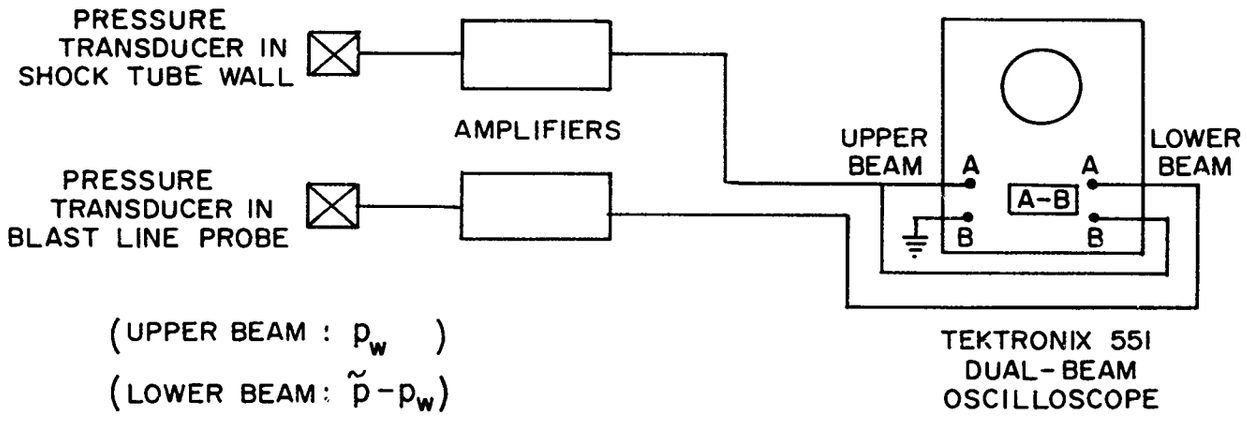

a) ELECTRONIC CIRCUIT

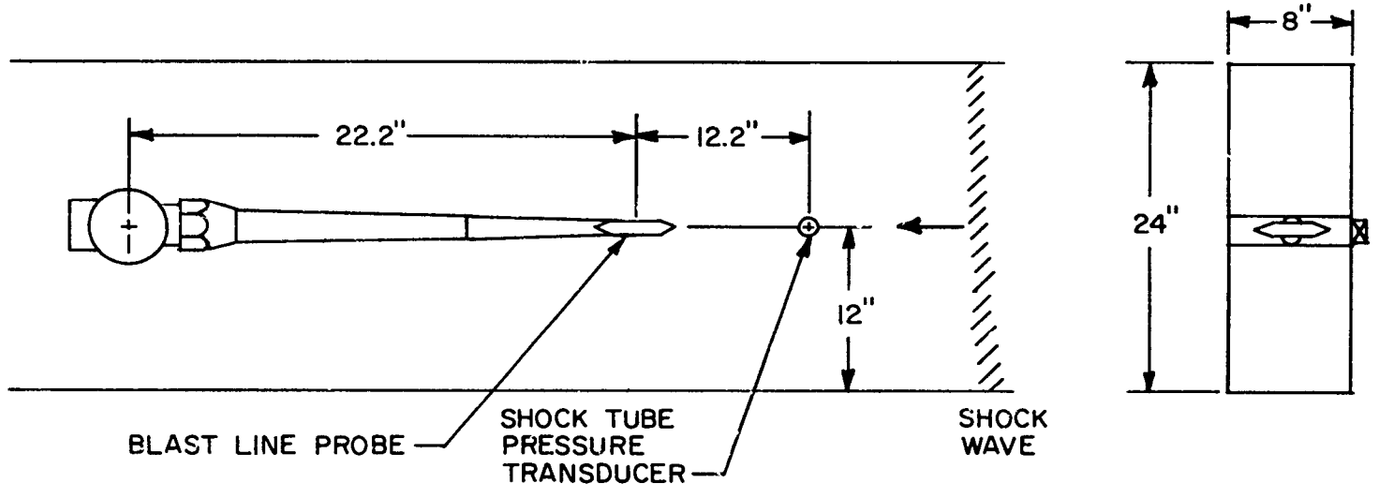

b) SHOCK TUBE ARRANGEMENT

Figure 4 Sketch of Arrangement for Calibration of Blast-Line Probe in Shock Tube

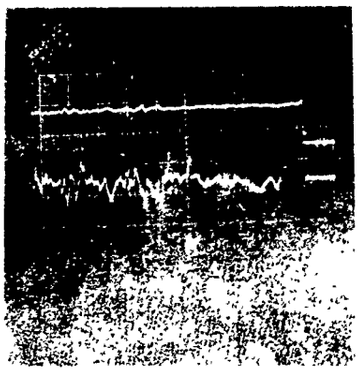

P_{21} = 1.24, M_2 = 0.237

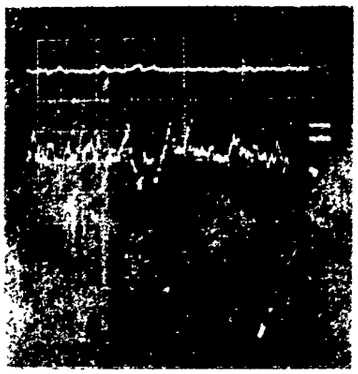

P_{21} = 1.62, M_2 = 0.335

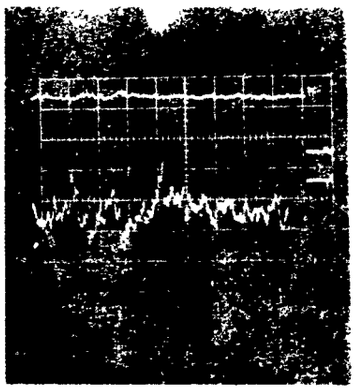

P_{21} = 2.08, M_2 = 0.500

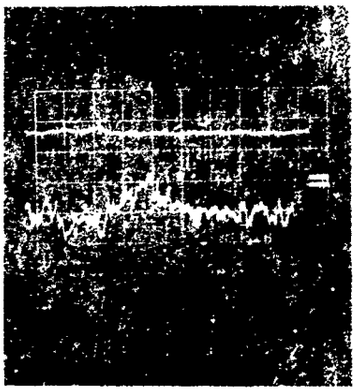

P_{21} = 2.40, M_2 = 0.650

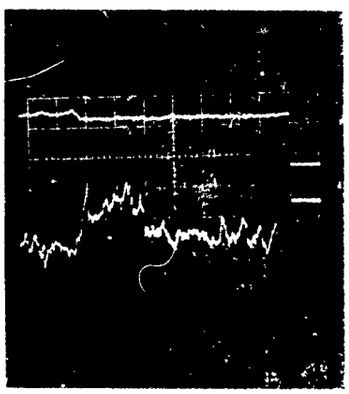

P_{21} = 2.91, M_2 = 0.709

Figure 5 Typical Oscillograph Records from Shock-Tube Calibration of Blast-Line Probe, P_1 = 31" Hg

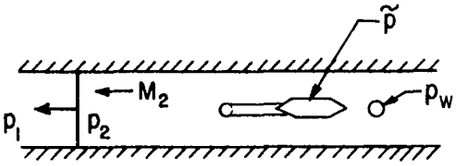

$\tilde{p}$ PRESSURE MEASURED BY PROBE
p_w PRESSURE AT SHOCK-TUBE WALL
p_1 PRESSURE IN FRONT OF SHOCK
p_2 PRESSURE BEHIND SHOCK
β_2 $\sqrt{1-M_2^2}$
M_2 MACH NUMBER BEHIND THE SHOCK
q DYNAMIC PRESSURE

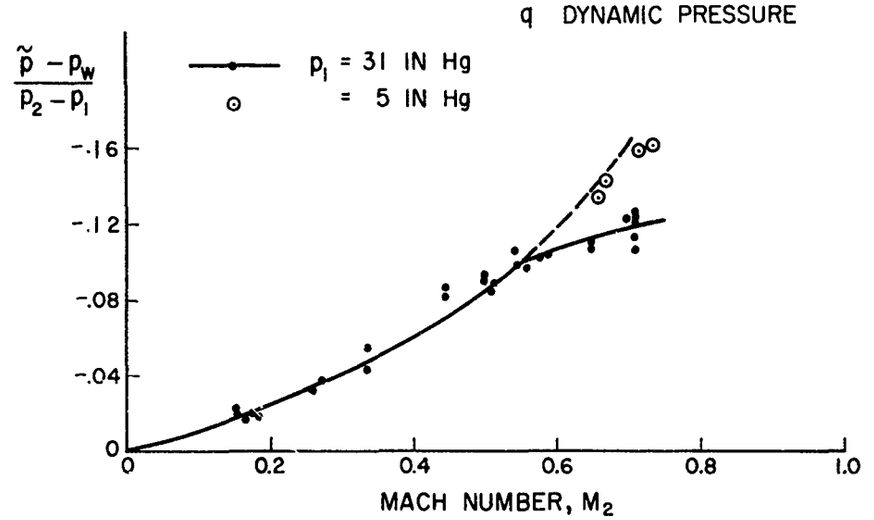

FIG. 6a

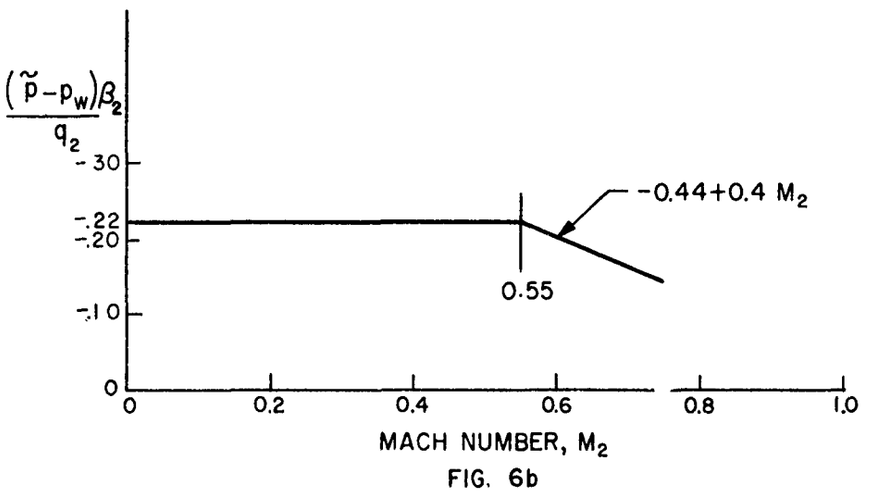

FIG. 6b

Figure 6 Calibration of Blast-Line Probe

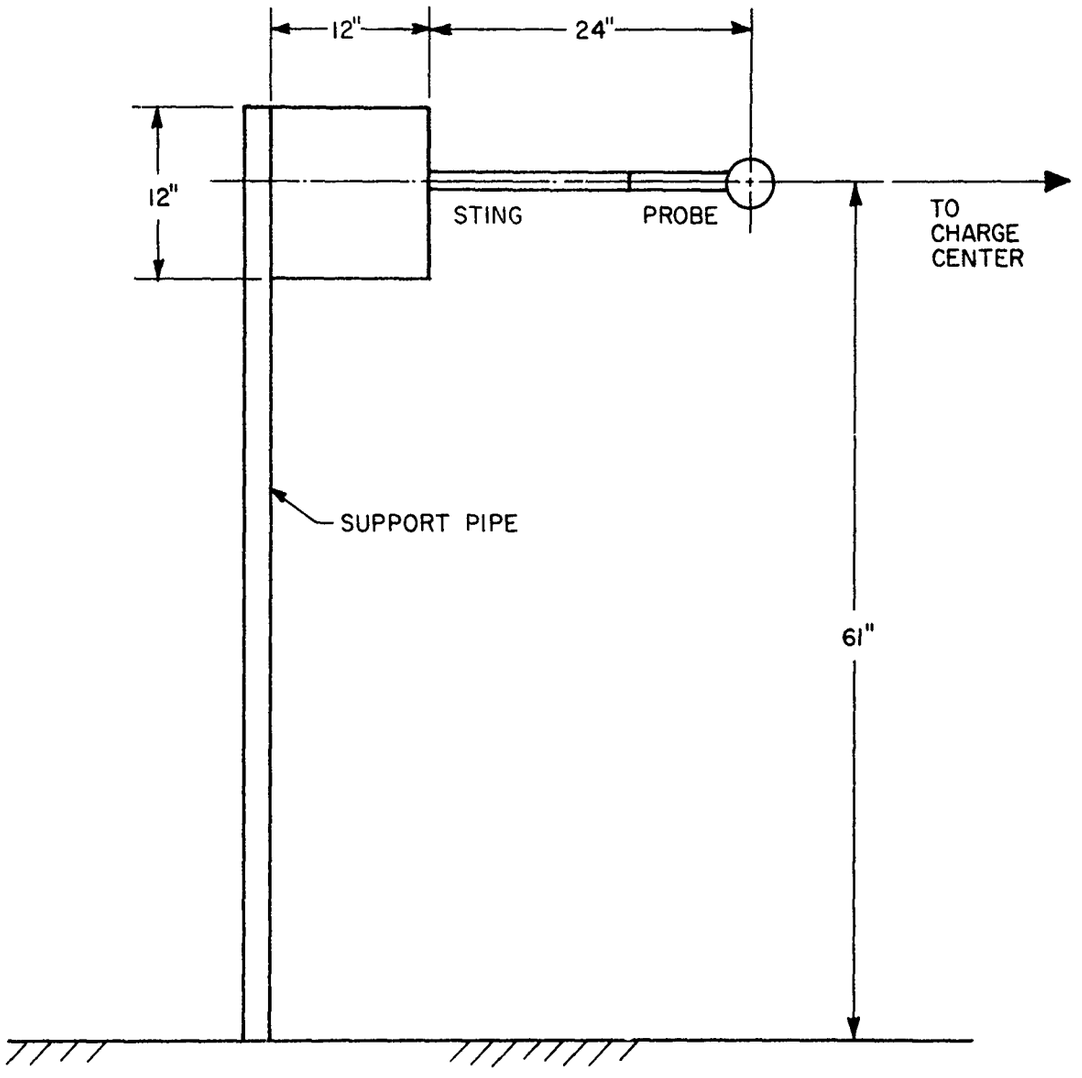

Figure 7 Sketch of a Typical Blast-Line Pressure Probe Installation

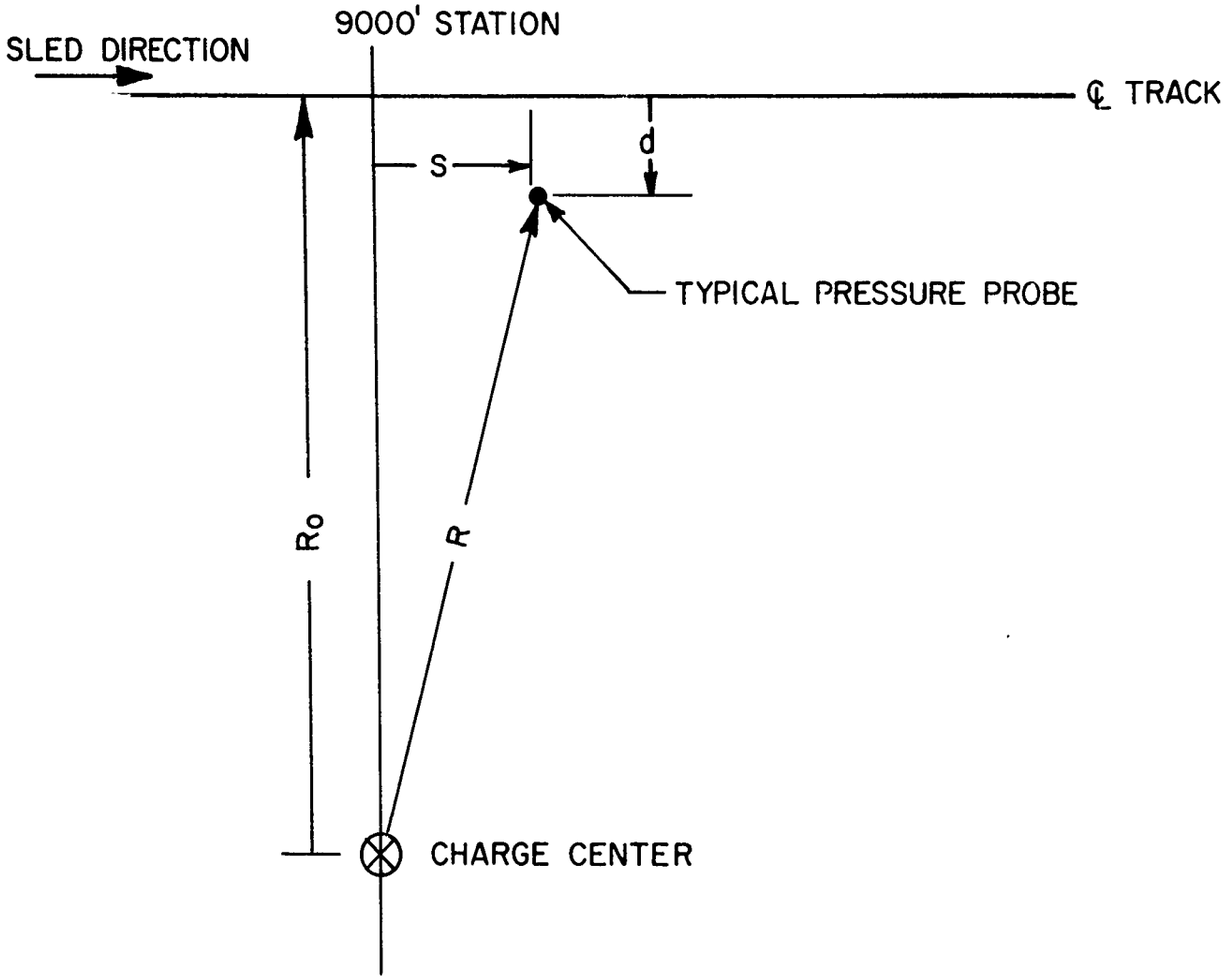

Figure 8 Sketch of Blast-Line and Sled Track

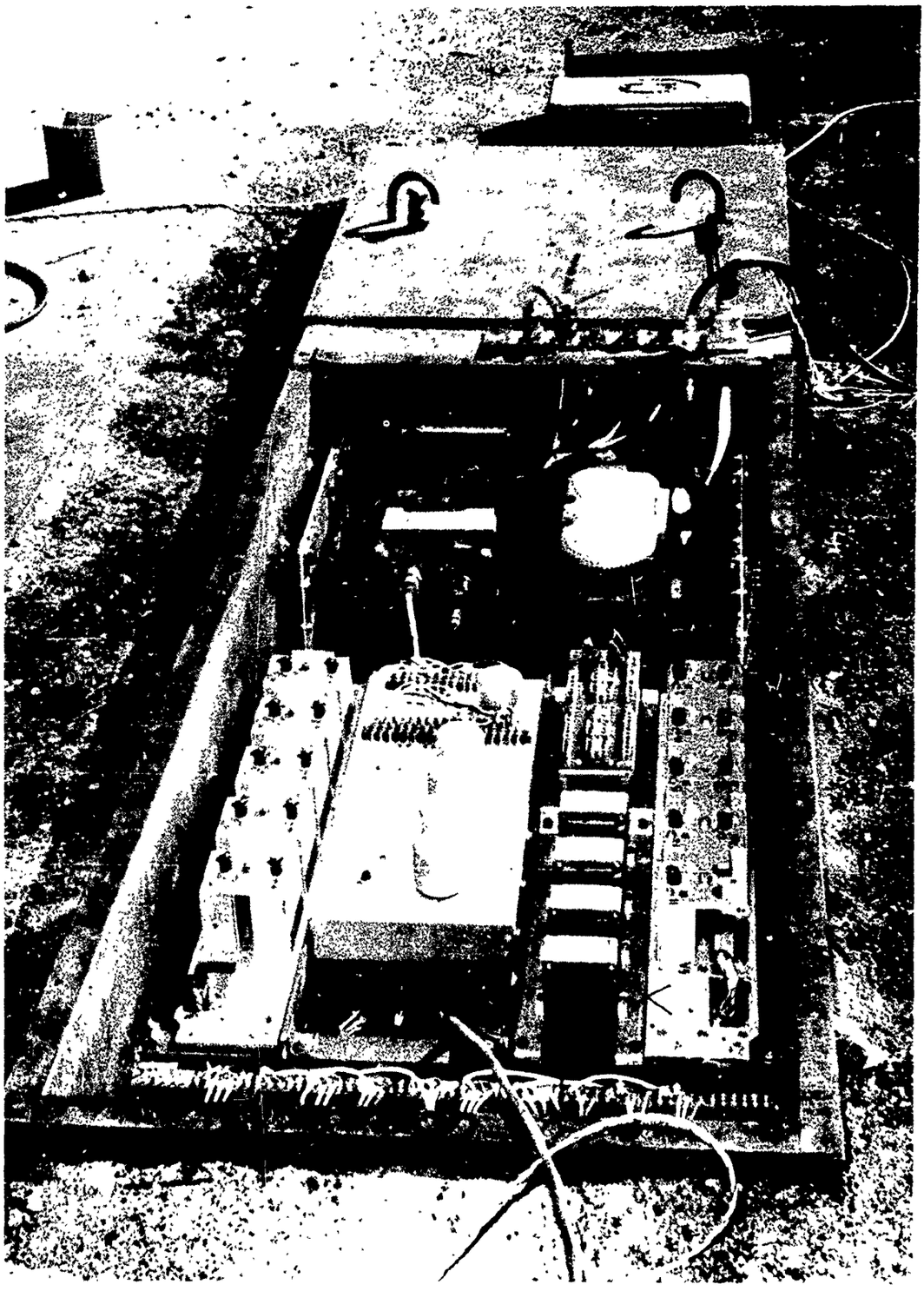

Figure 9 Photograph of Blast-Line Amplifier, Power Supply and Tape-Recorder Installation

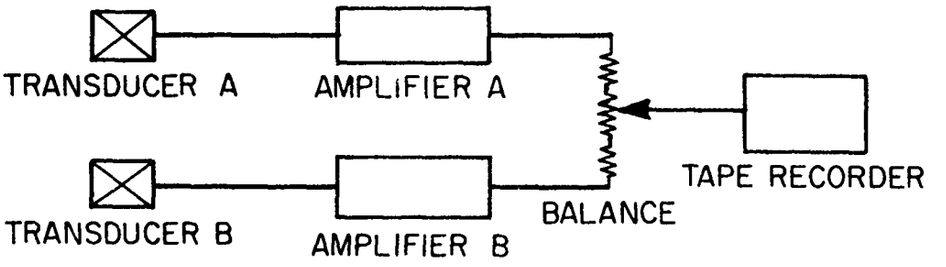

a. SCHEMATIC FOR MEASUREMENT OF OVERPRESSURE

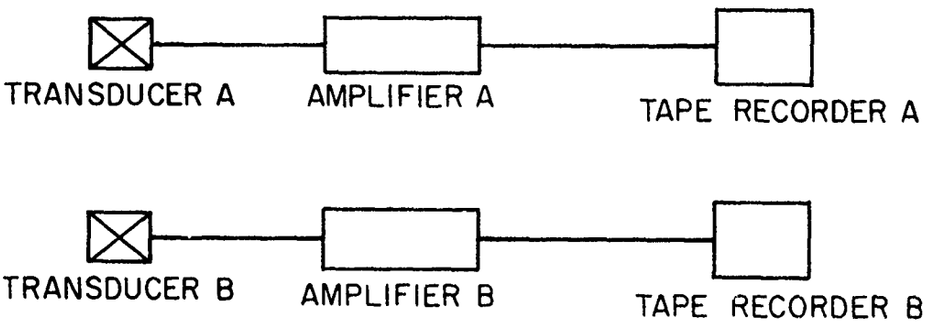

b SCHEMATIC FOR MEASUREMENT OF FLOW DIRECTION

Figure 10 Schematics of Electronic Circuits

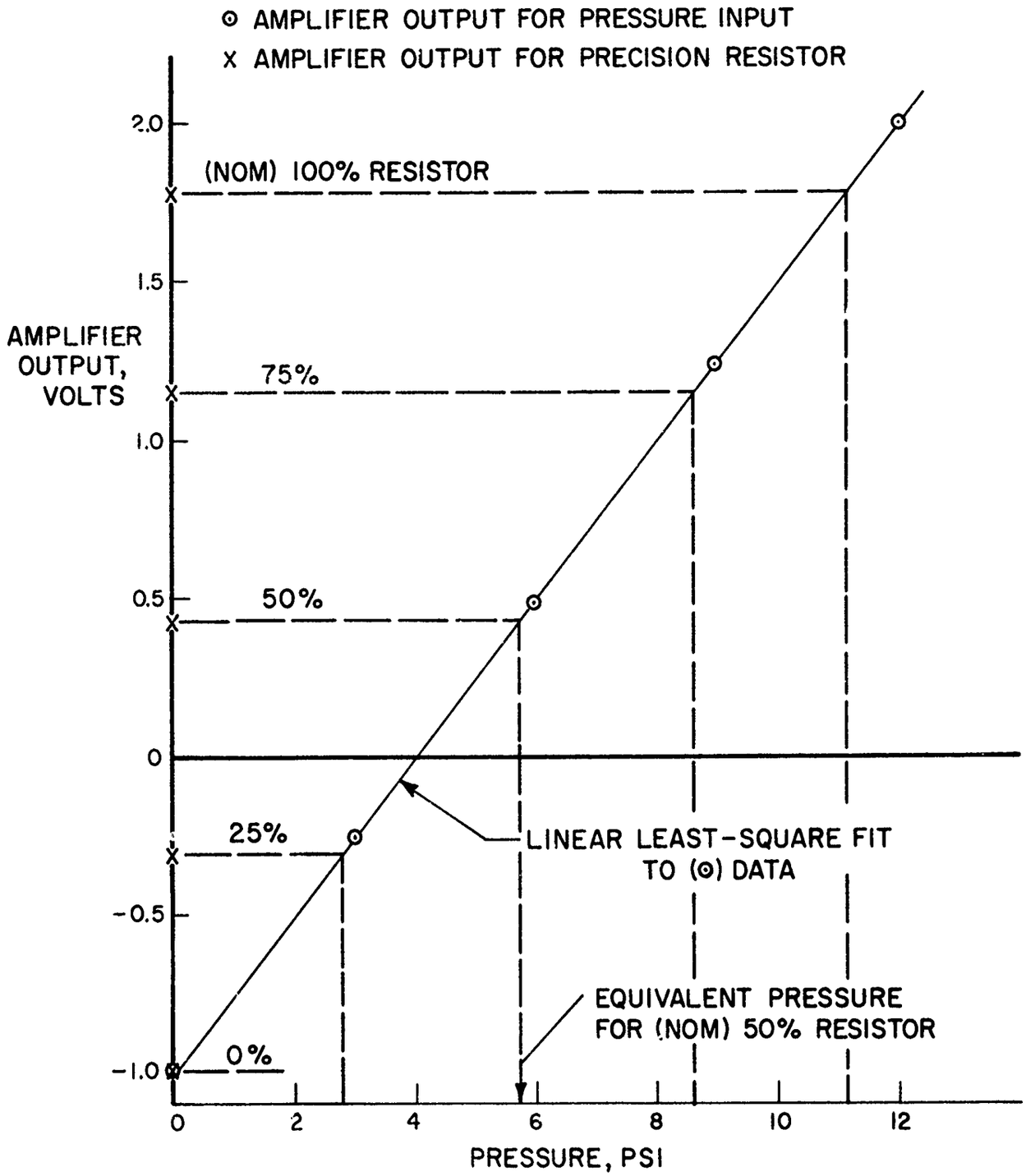

Figure 11 Typical Blast-Line Pressure Transducer Calibration

a. SIGNAL FROM BLAST-LINE-PROBE PRESSURE TRANSDUCER

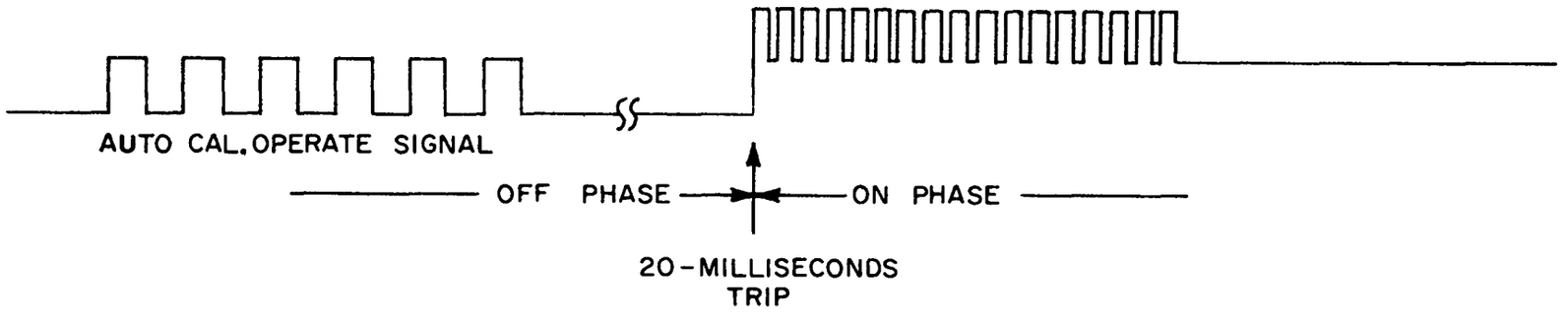

b. SIGNAL FROM TIME-CODE GENERATOR

Figure 12 Sketch of Typical Signals from a Blast-Line Tape Recorder

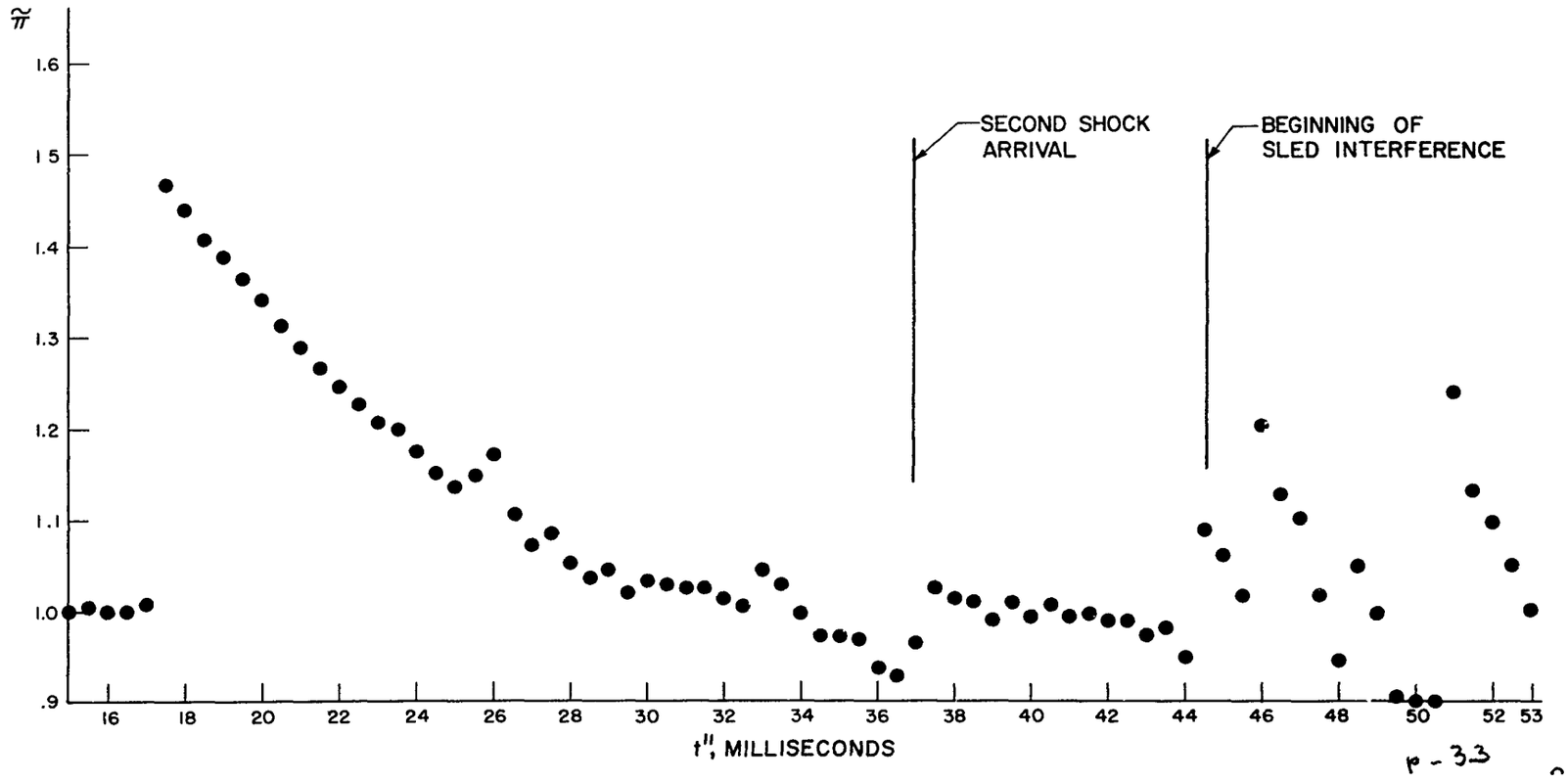

Figure 13 Measured Blast Overpressure, Data Run 4, Location S = +35 ft., d = +4.5 ft.

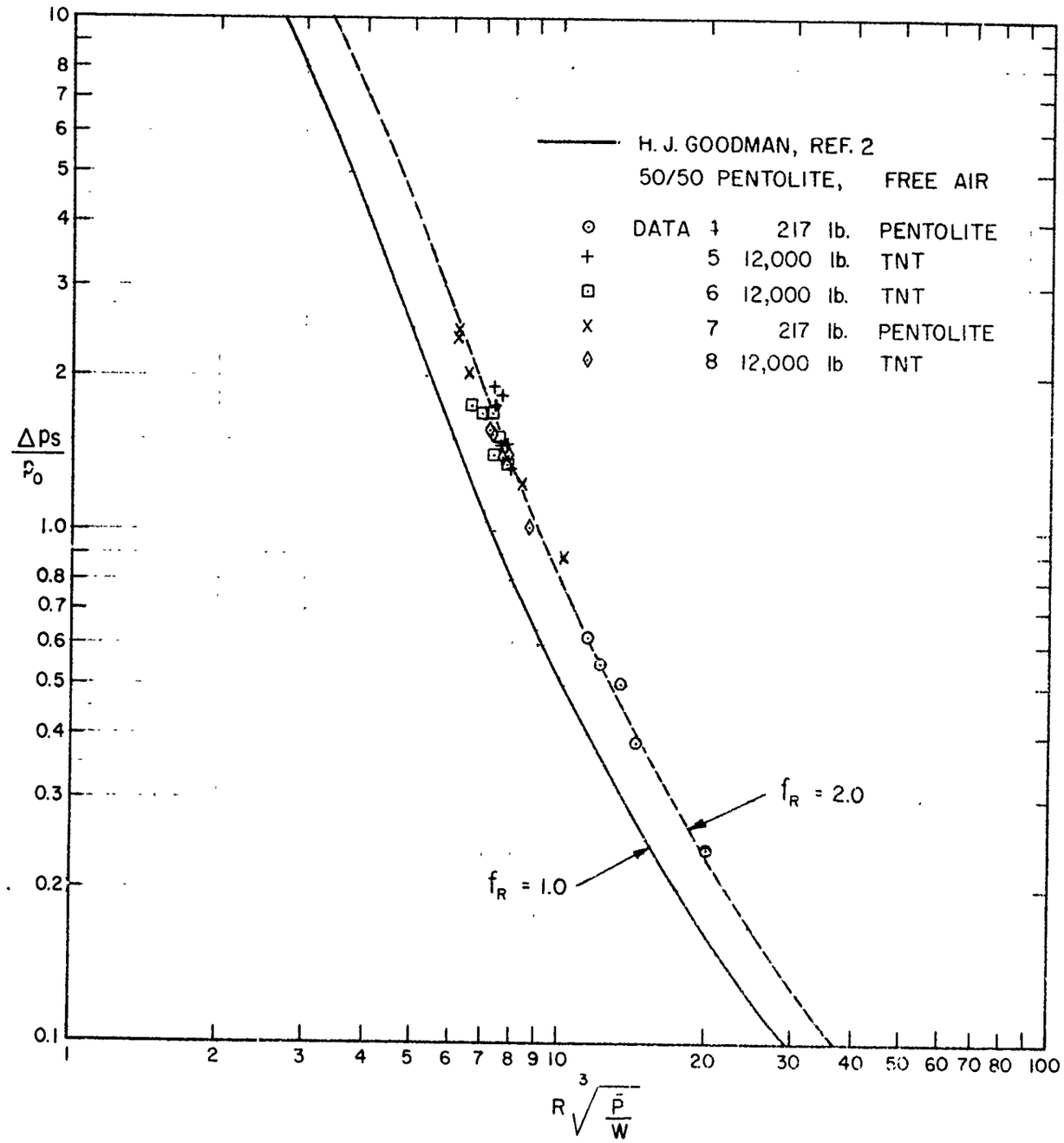

Figure 14 Shock Overpressure in BIG SEA Tests

TABLE 1

Blast-Line Gage Locations for the BIG SEA Program

No. (Position)	Support Pipe Location (S,d)	Run (Data No.) F2,F3	F5	F6	4	5	6	7	8
		Radius R from charge center to probe transducer, ft.							
1	(-10,20)	101.8	34.2	192.3					
2	(20,4.5)	118.8	52.3	208.8		178.5			178.5
3	(23,12)	112.2	47.7	201.8	70.5	171.5		38.1	171.5
4	(35,4.5)	122.5	59.4	211.0	81.9	180.6		51.4	180.6
5	(35,-5	132.5	69.3		92.3	191.8		60.9	191.8
6	(50,4.5)	127.6		214.0	89.3	184.3	163.2	62.5	184.3
7	(50,-5)			224.9			174.4		
8	(83,30)								
9	(93,16)						170.9	95.6	
10	(100,4.5)				123.9	203.3	184.5	106.0	203.3
11	(200,20)				207.4		243.0		
12	(400,20)						421.0		
13	(600,20)								
14	(800,20)								
15	(-10,4.5)	117.2	49.5	207.9	74.7	178.2	155.7	39.5	178.2
16	(10,4.5)	117.5	49.6	207.9	74.8	178.0	155.6	39.7	178.0
17	(8,12)	109.8	42.5	200.3	67.0	170.2	147.9	31.7	170.2
18	(17,12)	45.3							
19	(15,-5)	128.1	61.7	219.1	86.6	189.0	167.3	51.8	189.0
20	(0,6)	116.3	48.7						

TABLE 2

Shock Data for BIG SEA Tests*

Run	F6	4	5	6	7	8
Charge description	TNT	Pent.	TNT	TNT	Pent.	TNT
Charge weight, lb.	12000	216	12000	12000	216	12000
Distance from track centerline to charge, ft.	213.8	81.3	185.0	162.8	45.7	184.2
p_o	13.716	13.576	13.632	13.539	13.627	13.519
f_R	2.41	2.11	2.15	2.01	2.08	2.07
π_S	2.01	1.48	2.24	2.66	2.52	2.28
η_S	1.59	1.32	1.77	1.93	1.89	1.77
β_S	0.54	0.27	0.64	0.79	0.73	0.63
$\Delta t_{+\Delta p}$ (9000 ft. sta)	50	16	34	35	8.9	38
std.dev.$[1 - \frac{\Delta p(\text{meas})}{\Delta p(\text{Goodman})}]$	4.7	3.7	4.7	6.6	6.0	3.6

- - - - - - - - - - - - - - - - -

* Data are deleted for tests in which stacked 8-lb. blocks of TNT in aggregate of 216 lbs. were employed, since the associated blast fields appear to lack repeatability and symmetry.

Unclassified
Security Classification

DOCUMENT CONTROL DATA - R&D

(Security classification of title, body of abstract and indexing annotation must be entered when the overall report is classified)

1. ORIGINATING ACTIVITY (Corporate author)	2a REPORT SECURITY CLASSIFICATION
Massachusetts Institute of Technology (ASRL) Cambridge, Massachusetts 02139	Unclassified
	2b GROUP

3 REPORT TITLE

Pressure Probe and System for Measuring Large Blast Waves

4. DESCRIPTIVE NOTES *(Type of report and inclusive dates)*

Technical Report

5 AUTHOR(S) *(Last name, first name, initial)*

Ruetenik, J. Ray
Lewis, S. Dean

6. REPORT DATE	7a TOTAL NO. OF PAGES	7b. NO OF REFS
June 1965	36	5

8a CONTRACT OR GRANT NO.	9a. ORIGINATOR'S REPORT NUMBER(S)
AF 33(616)-8499	AFFDL-TDR-65-35
b. PROJECT NO. 5710	
c.	9b. OTHER REPORT NO(S) *(Any other numbers that may be assigned this report)*
d.	ASRL TR 105-2

10 AVAILABILITY/LIMITATION NOTICES

Qualified requestors may obtain copies of this report from DDC and/or OTS.

11. SUPPLEMENTARY NOTES	12. SPONSORING MILITARY ACTIVITY
	Air Force Flight Dynamics Laboratory (AFFDL/FDTR)

13 ABSTRACT

A new pancake-type pressure probe was developed for the measurement of blast pressure waves during the BIG SEA sled tests. This probe employs transducers of the type selected for wing pressure measurements in that program. It was evaluated in the shock tube under a range of flow Mach numbers encountered during the test. From these shock tube tests, a probe form calibration was determined.

Application of this type of probe to the BIG SEA tests is also described, including the mounting system, transducer and electronic calibration, and one blast wave record derived from this type of probe is presented. The results of the shock-overpressure measurements are compared with other test data.

The pancake probe has a diameter of 4 inches and a thickness of 0.5 inch. The accuracy of measurement has been determined to be 3-5% of the shock overpressure for blast waves where the positive duration is 10 milliseconds or greater. The response time has been found to be less than 0.7 milliseconds.

DD FORM 1 JAN 64 1473

Unclassified
Security Classification

Unclassified
Security Classification

14. KEY WORDS	LINK A		LINK B		LINK C	
	ROLE	WT	ROLE	WT	ROLE	WT
Blast wave measurements **Pressure probe** **Transient pressure measurement**						

INSTRUCTIONS

1. ORIGINATING ACTIVITY: Enter the name and address of the contractor, subcontractor, grantee, Department of Defense activity or other organization *(corporate author)* issuing the report.

2*a*. REPORT SECURITY CLASSIFICATION: Enter the overall security classification of the report. Indicate whether "Restricted Data" is included. Marking is to be in accordance with appropriate security regulations.

2*b*. GROUP: Automatic downgrading is specified in DoD Directive 5200.10 and Armed Forces Industrial Manual. Enter the group number. Also, when applicable, show that optional markings have been used for Group 3 and Group 4 as authorized.

3. REPORT TITLE: Enter the complete report title in all capital letters. Titles in all cases should be unclassified. If a meaningful title cannot be selected without classification, show title classification in all capitals in parenthesis immediately following the title.

4. DESCRIPTIVE NOTES: If appropriate, enter the type of report, e.g., interim, progress, summary, annual, or final. Give the inclusive dates when a specific reporting period is covered.

5. AUTHOR(S): Enter the name(s) of author(s) as shown on or in the report. Enter last name, first name, middle initial. If military, show rank and branch of service. The name of the principal author is an absolute minimum requirement.

6. REPORT DATE: Enter the date of the report as day, month, year, or month, year. If more than one date appears on the report, use date of publication.

7*a*. TOTAL NUMBER OF PAGES: The total page count should follow normal pagination procedures, i.e., enter the number of pages containing information.

7*b*. NUMBER OF REFERENCES: Enter the total number of references cited in the report.

8*a*. CONTRACT OR GRANT NUMBER: If appropriate, enter the applicable number of the contract or grant under which the report was written.

8*b*, 8*c*, & 8*d*. PROJECT NUMBER: Enter the appropriate military department identification, such as project number, subproject number, system numbers, task number, etc.

9*a*. ORIGINATOR'S REPORT NUMBER(S): Enter the official report number by which the document will be identified and controlled by the originating activity. This number must be unique to this report.

9*b*. OTHER REPORT NUMBER(S): If the report has been assigned any other report numbers *(either by the originator or by the sponsor)*, also enter this number(s).

10. AVAILABILITY/LIMITATION NOTICES: Enter any limitations on further dissemination of the report, other than those imposed by security classification, using standard statements such as:

(1) "Qualified requesters may obtain copies of this report from DDC."

(2) "Foreign announcement and dissemination of this report by DDC is not authorized."

(3) "U. S. Government agencies may obtain copies of this report directly from DDC. Other qualified DDC users shall request through _____."

(4) "U. S. military agencies may obtain copies of this report directly from DDC. Other qualified users shall request through _____."

(5) "All distribution of this report is controlled. Qualified DDC users shall request through _____."

If the report has been furnished to the Office of Technical Services, Department of Commerce, for sale to the public, indicate this fact and enter the price, if known.

11. SUPPLEMENTARY NOTES: Use for additional explanatory notes.

12. SPONSORING MILITARY ACTIVITY: Enter the name of the departmental project office or laboratory sponsoring *(paying for)* the research and development. Include address.

13. ABSTRACT: Enter an abstract giving a brief and factual summary of the document indicative of the report, even though it may also appear elsewhere in the body of the technical report. If additional space is required, a continuation sheet shall be attached.

It is highly desirable that the abstract of classified reports be unclassified. Each paragraph of the abstract shall end with an indication of the military security classification of the information in the paragraph, represented as *(TS)*, *(S)*, *(C)*, or *(U)*.

There is no limitation on the length of the abstract. However, the suggested length is from 150 to 225 words.

14. KEY WORDS: Key words are technically meaningful terms or short phrases that characterize a report and may be used as index entries for cataloging the report. Key words must be selected so that no security classification is required. Identifiers, such as equipment model designation, trade name, military project code name, geographic location, may be used as key words but will be followed by an indication of technical context. The assignment of links, rules, and weights is optional.

Unclassified
Security Classification